Sensitivity and Dynamic Range Considerations for Homodyne Detection Systems

Jaggard, Dwight L.; King, Ray J

Link back to DTU Orbit

Sensitivity and Dynamic Range Considerations for Homodyne Detection Systems

DWIGHT L. JAGGARD, STUDENT MEMBER, IEEE, AND RAY J. KING, MEMBER, IEEE

Abstract—The effects of modulation frequency, RF reference power, and external bias upon the sensitivity and dynamic range of microwave homodyne detection systems was measured for point contact diodes and low $1/f$ noise Schottky and backward diodes. The measurements were made at 4.89 GHz using a signal to noise ratio of 3 dB and a detection system bandwidth of 10 Hz. Maximum sensitivities of -135, -150, and -145 dBm, and dynamic ranges of 92, 110, and 124 dB were measured for the point contact, Schottky, and backward diodes at modulation frequencies of 30, 30, and 3 kHz, respectively. It was found that the level of RF reference signal needed to obtain the maximum sensitivity was equal to or somewhat above the point where the diode changes from square law to linear detection. The results are significant in that previously reported homodyne sensitivities (not necessarily maximum) were on the order of -90 to -130 dBm for point contact diodes and no data are available for Schottky and backward diodes. Significantly improved stability, sensitivity, and dynamic range can be achieved using these low $1/f$ noise devices, the correct external bias, and the optimum RF reference power.

I. INTRODUCTION

H OMODYNE (synchronous) detection is a process whereby a modulated signal which is to be detected is mixed with a CW reference signal of the same frequency in a nonlinear device, and the output signal is bandpass filtered. The detection process is basically the same as heterodyne detection except that the intermediate frequency (IF) is zero, and the detected signal generally lies in the audio range. Low-frequency detector noise therefore plays a dominant role and conventional methods of specifying mixer diode characteristics are usually not very useful.

Although comparisons of the operational characteristics of various devices for video and heterodyne detection have appeared [1]-[5], little attention has been given to the operational characteristics of these devices when used as homodyne detectors. Notable exceptions are the papers by Brodwin *et al.* [6], who studied the sensitivity characteristics of point contact detectors as a function of reference signal amplitude, and by

Mathers [7], Richmond [8], and O'Brien [9] who have given typical sensitivities which were obtained using either point contact diodes or barretters. These early papers gave little attention to such questions as the behavior of diode $1/f$ or "flicker" noise at low frequencies and the effect of externally applied bias when detecting in the homodyne mode. Also, Schottky and backward diodes are two additional very useful low noise detecting devices, and no evaluation of their homodyne detection characteristics has been made. To satisfy this need we have attempted to establish criteria for evaluating these three different diode types by investigating the quantitative effects of externally applied bias, modulation frequency, and reference signal level upon the sensitivity and dynamic range of homodyne detection systems. These parameters were studied using a radio frequency of 4.89 GHz. Although the results depend to some degree upon the radio frequency, the particular diode, its mount, and associated bias and output circuitry, they are generally adequate to show how the sensitivity and dynamic range of the homodyne detector can be maximized.

The results show maximum sensitivities S_m on the order of -135, -150, and -145 dBm and maximum dynamic ranges D_m of 92, 110, and 125 dB for the point contact, Schottky, and backward diodes at modulation frequencies of 30, 30, and 3 kHz, respectively, using a bandwidth of 10 Hz. The sensitivity values for the point contact diode are 5 to 45 dB better than previously reported results [6]-[9].

II. THEORY

Consider two signals of the same radian frequency ω where

$$V_r = Ae^{j\omega t} \tag{1}$$

$$V_i = b(1 + m \cos \omega_m t) e^{j(\omega t + \phi)}. \tag{2}$$

The CW reference signal V_r is of amplitude A, the information signal V_i is of amplitude b and is double-sideband with carrier (DSBWC) amplitude modulated with modulation index m. The radian modulation frequency is ω_m ($\omega_m \ll \omega$), and V_i differs in phase from V_r by phase angle ϕ. Using the phasor diagram shown in Fig. 1, and noting that at low levels the detector has a square-law response, the output is proportional to $E_t^2 (= (V_r + V_i)^2$. Thus using the law of cosines and retaining only those terms at ω_m, the detected output is

$$V_0 = K_l Abm \left(\frac{b}{A} + \cos \phi \right) \cos \omega_m t \tag{3}$$
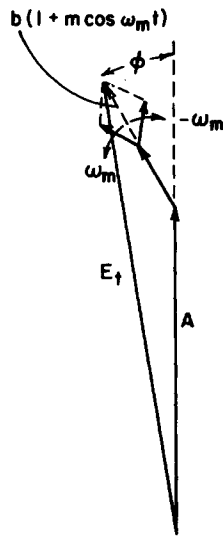
Fig. 1. Phasor diagram showing addition of reference signal A and DSBWC amplitude modulated information signal to yield total signal E_t arriving at detector.

where K_l is the low level gain constant. The b/A term in (3) represents the effect of the unsuppressed carrier in the information signal which is given by the first term in (2), and contributes to both phase [10]-[12] and amplitude measurement errors [11], [13], [14]. Its presence is most objectionable when making phase measurements, wherein ϕ is adjusted in one of the channels by using a phase shifter so that (3) is nulled. The phase error can be made negligible small by requiring $b \ll A$, e.g., for $b/A < -30$ dB the phase error is less $1.8°$. Thus the amount of phase error which can be tolerated determines the lower level of A which in turn determines the upper bound on the dynamic range of b. In the following we shall assume that $b/A < -30$ dB, and so the first term in (3) can be ignored. Alternatively, by using a balanced modulator and/or mixer, a multiplying suppression factor will be introduced to reduce this error term [11], [12]. Similar errors using single sideband modulation have also been analyzed [11].

At higher levels of A, the detector characteristic becomes linear and simply detects the *envelope* of the total input E_t. For $b \ll A$, the output portion of E_t at ω_m is

$$V_0 = K_h bm \cos \phi \cos \omega_m t \qquad (4)$$

where K_h is the high level gain constant. The important difference between (3) and (4) is that the output for linear detection is not a function of the reference signal amplitude A whereas for square-law detection (3) shows that the output is a linear function of A [6], [11]. In either case, the output is directly proportional to $b \cos \phi$ (assuming $b \ll A$) and can therefore be used to make phase and amplitude measurements on the information channel signal arriving at the detector. Here we are only concerned with the dynamic range of b and the ability of the system to measure small values of b, i.e., sensitivity, and so we shall always set $\cos \phi = 1$.

Aside from the errors in phase and amplitude introduced by not having $b \ll A$, a second type of measurement error can occur due to unwanted signals, e.g., leakage or reflection of a

portion of the modulated information signal into the reference channel or vice versa. These errors can be minimized by using isolators, circulators, well matched magic tees, directional couplers, attenuators, and tuners.

The effect of the reference channel signal level A, the detector noise and externally applied bias, and the modulation frequency ω_m, are all important in homodyne detection. A should be large since a large dynamic range of b is desired, and since $b \ll A$ must hold for error free phase measurements. But very large values can damage the diode, cause large losses due to extreme impedance mismatch, or cause the rectified signal current to develop a reverse self-bias through the dc load resistance. Another disadvantage arises from the increased low-frequency noise generated within the detector. Since the output becomes independent of A at high levels, a point is reached beyond which further increases in A simply increase the conversion loss or add noise with a corresponding reduction in the output signal to noise ratio. On the other hand, when A is decreased into the square-law region, the detected signal output decreases in direct proportion to A. Since the detector noise is at its lowest value and essentially constant, the net result is again a reduction in the output signal to noise ratio. *An optimum value of A can therefore be found near or somewhat above the transition region from square-law to linear detection which will give the maximum sensitivity S_m.* This point will be dependent upon diode type and mount, external bias and bias circuit impedance, and modulation frequency. Furthermore, it will be necessary to determine the tradeoffs which can be made to yield the greatest dynamic range in b.

Most readers are familiar with the characteristics of point contact diodes when used as mixers [15], [16] and so the mixing characteristics of the Schottky and backward diodes will be briefly compared with this device. More comprehensive comparisons are available [1], [3], [4]. First the advantages: because construction of the Schottky and backward diodes does not involve a metal whisker-semiconductor junction, *they are inherently more stable with temperature and mechanical vibrations, have a higher burnout rating, and can be operated at higher local oscillator power levels (A for homodyne applications) without significantly increasing the diode noise.* Still another advantage is that Schottky and backward diodes generate significantly *lower noise (10 to 30 dB) at low IF* (IF is zero for homodyne). The point contact diode has a $1/f$ noise power spectrum below the noise corner which lies between 100 kHz and 1 MHz. Above the noise corner the noise is almost entirely shot and thermal which are constant for frequencies up to 10^8 and 10^{13} Hz, respectively, and in the range the noise from the Schottky and backward diodes is comparable to the point contact [1], [4], [17]. More importantly for homodyne applications, the Schottky diode also has a $1/f$ noise spectrum but has a considerably lower noise corner which varies from 50 Hz to 30 kHz, while the backward diode noise generally increases more slowly than $1/f$ as the frequency is reduced, and the noise corner can be as low as 1 kHz.

In the disadvantages column, the Schottky diode requires a small amount of external bias to conduct at low local oscillator power levels (A). Otherwise the Schottky and point

contact diodes have comparable IF impedances (100 to 500 Ω) and in many cases the Schottky can be used as a direct replacement for the point contact. However, special detector design considerations are required for the backward diode which is usually operated with zero bias and a very low impedance dc load. Furthermore, the IF impedance is quite low (40 to 100 Ω), and so a special IF amplifier is usually needed, e.g., transformer [4] or low impedance transistor amplifier [5].

Rough calculations using well-known formulas for receiver sensitivity give maximum sensitivity values of $-127, -149$, and -153 dBm for the point contact, Schottky, and backward diodes, respectively, at a modulation frequency of 1 kHz. These values compare favorably with the experimental results.

III. THE EXPERIMENT

Fig. 2 shows the C-band (3.95 to 5.85 GHz) microwave homodyne detection system that was used in the following experiments. The CW signal from the 1.5-W klystron was divided into the reference and information channels by magic tee No. 1 which in conjunction with tuner T_1, isolators, and attenuators in each channel, provided a high degree of isolation between channels. The reference channel provided a reference signal V_r of amplitude A, while the information channel provided a DSBWC amplitude modulated ($m = 0.6$) signal V_i of amplitude b (see (1) and (2)). These signals were combined by magic tee No. 2, which, in conjunction with tuner T_2 provided additional isolation between channels. The variable attenuators set the power levels so that $b \ll A$. The position of the slotted line probe determined the phase angle ϕ between V_r and V_i, and was always adjusted so that $\cos \phi = 1$. Since $A \gg b$, V_r synchronously switches the detector diode, giving an output of the form of (3) or (4).

The detector mount was coaxial and tunable with a dc return. It was observed that the optimum tuning of the mount was not measureably changed for levels of A below or somewhat above that which gave maximum sensitivity, and so the tuning was performed for $A \cong -10$ dBm and held fixed for each diode at each external bias setting. The bias circuit had an internal impedance of 100 k Ω, capable of supplying up to 1 mA external bias. The chosen bias current remained constant until A exceeded its optimum value by about 5-10 dB.

The medium impedance low-noise preamplifier provided a voltage gain of 100 and had an input resistance of 100 k Ω. This preamplifier, model 148L by Ithaco, was used for the point contact and Schottky diodes and had a noise figure of 4 dB for a source resistance of 200 Ω at 30 kHz. The addition of a resistive load in parallel with the preamplifier input only degraded the sensitivity and made the diode response more dependent upon the level of A. Therefore, no additional external shunting load was used for any of the diode types.

The low impedance low noise preamplifier which was used for the backward diode provided a voltage gain of 1000 and had a dc resistance of 2 Ω due to the transformer coupled input. The preamplifier, model G1 by Ithaco, had a noise figure of 0.5 dB for a source resistance of 75 Ω at 300 Hz, and provided the proper resistive load and near zero bias.
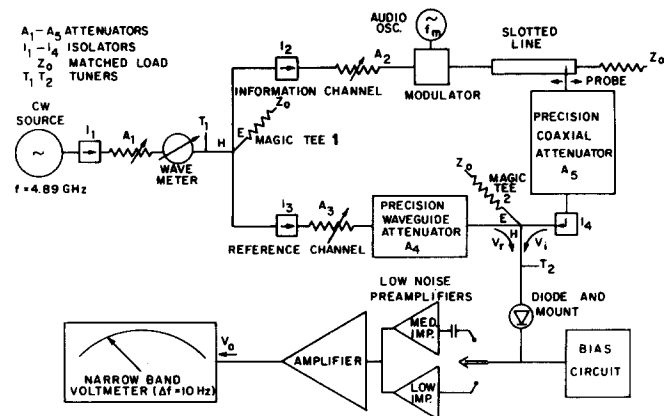
A compensated thermister bridge and power meter were

Fig. 2. Microwave homodyne system for testing detection characteristics of various diode types.

used to establish the power level of each channel at the detector mount and the precision attenuators were used to vary A from +10 to -40 dBm and vary b from -90 to -140 dBm for the point contact, or from -110 to -160 dBm for the more sensitive Schottky and backward diodes.

The first data taken from the point contact and Schottky diodes established the minimum detectable signal b which was 3 dB above noise as a function of A in the range $-40 < A < +10$ dB using external bias as the parameter. This gave information needed to determine the optimum bias. The modulation frequency f_m was held fixed at 1 kHz, and the bandwidth Δf at 10 Hz.

Next, data were taken to determine the output for fixed b ($=-70$ dBm) versus A using external bias as the parameter, and a fixed modulation frequency of 1 kHz. These results established the detector square law, transition, and linear response regions as a function of A and external bias. These regions are defined according to whether the output slope was +1 for the square-law region or zero for the linear region, and the transition region was where the slope deviated more than 1 dB from these values. The results of this second part of the experiment were used to correlate the center of the transition region with A_0, the optimum value of A which occurred at the point of maximum sensitivity as previously suggested in Section II.

In the third part of the experiment the minimum detectable signal b was measured as a function of A over the range $-40 < A < +10$ dBm, using the modulation frequency between 100 Hz and 30 kHz as a parameter and the optimum bias found from the first data. This established the maximum sensitivity S_m and maximum dynamic range of b, D_m, as functions of A and modulation frequency f_m.

In all of these experiments, errors due to attenuator settings and unsteady meter readings were of the order of ± 0.25 dB for A and ± 1.0 dB for b.

IV. EXPERIMENTAL RESULTS

Two new notations will be useful in this and the following sections. For a given modulation frequency and external bias, A_d refers to the value of A where the maximum dynamic range D_m occurs, while A_{TR} denotes the approximate center of the transition region.
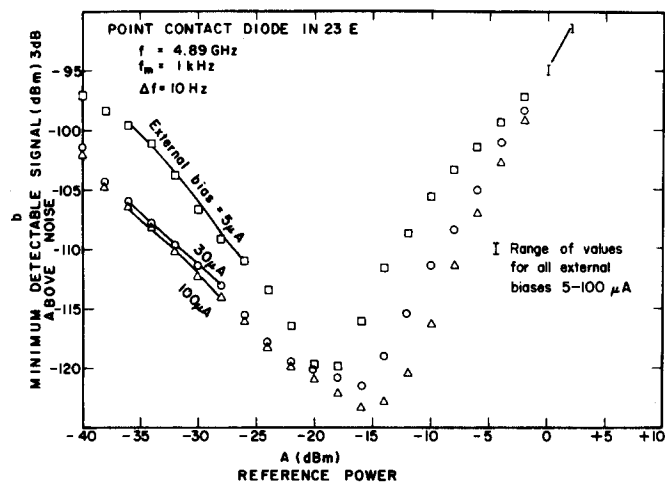
Fig. 3. Minimum detectable signal versus A with external bias as parameter for point contact diode.
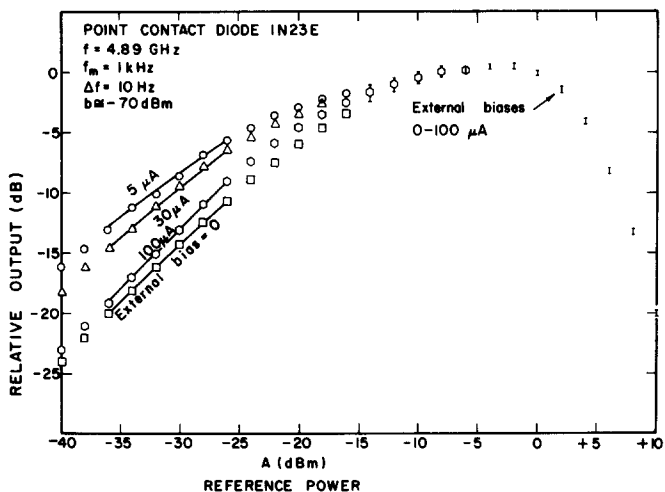

Fig. 4. Relative output of point contact diode versus A with external bias as parameter and fixed information signal input (-70 dBm).
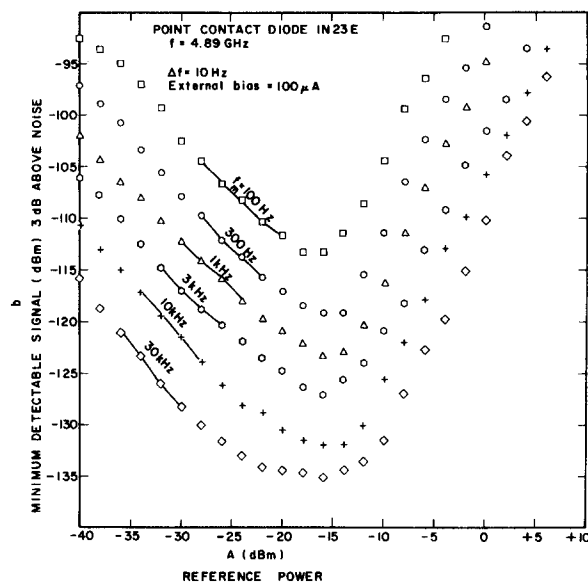

Fig. 5. Minimum detectable signal for point contact diode versus A with fixed external bias and modulation frequency f_m as parameter.

TABLE I
MAXIMUM SENSITIVITY AND DYNAMIC RANGE AS FUNCTION OF
MODULATION FREQUENCY FOR 1N23E CONTACT DIODE

f_m (Hz)	Maximum Sensitivity S_m(dBm)	A_o (dBm)	Maximum Dynamic Range D_m(dB)	A_d (dBm)
100	-113	-17	67	-14
300	-119	-16	74	-14
1 k	-123	-16	79	-14
3 k	-127	-16	82	-13
10 k	-132	-16	88	-12
30 k	-135	-16	92	-11

A. Point Contact Diode

Figs. 3-5 show the results of the three experimental procedures outlined previously using the point contact diode. For f_m = 1 kHz, Fig. 3 shows the minimum detectable signal as a function of A with external bias as a parameter. It is apparent that increasing the external bias increases both the maximum sensitivity and the dynamic range. It was observed that no improvement in maximum sensitivity could be realized by increasing the bias above 100 μA, and so curves for larger bias are not shown.

The upswing of the curves in Fig. 3 for $A > A_0$ is largely due to the onset of reverse self-bias which was caused by the flow of rectified RF current through the 100 k Ω internal resistance of the bias circuit. Of course, increased diode noise also plays a role. Consequently, if measures are taken to eliminate or compensate the reverse self-bias, these curves would display a somewhat broader minimum which would extend to higher values of A. This broadening would probably not improve the observed maximum sensitivity, but would increase the maximum dynamic range since A could then be set somewhat above the optimum A_0 as measured from Fig. 3.

Unfortunately, this reverse self-bias effect was not noticed until shortly before the final paper was due for printing, and so it was not possible to repeat the experiments to observe the increased dynamic range which could be achieved. However, additional data are planned for a future note.

Fig. 4 shows the output of the diode as the level of A is varied again using external bias as a parameter. For the 100-μA curve, the detector is square-law for $A < -22$ dBm, in the transition region for -22 dBm $< A < -11$ dBm and linear for -11 dBm $< A < +1$ dBm. Note the broad transition region between the square-law and linear detection regions, especially for small bias. For $A < 0$ dBm the reverse self-bias is not important here since the signal b (= -70 dBm) is well above the noise level. However, its effect is quite pronounced for $A > 0$ dBm where the sharp drop-off in detected output is observed.

For homodyne systems, operation is normally in the region where the curves in Fig. 4 begin to merge. Consequently, bias should be chosen on the basis of maximum sensitivity and not maximum output. According to Fig. 3, the optimum bias for the point contact diode was therefore taken as 100 μA in Fig. 5 which shows the minimum detectable signal as a function of A using f_m as the parameter. Table I summarizes the results shown in Fig. 5.

In Table I, A_d has been taken at the point where the slope

begins to be greater than +1 and is therefore always somewhat greater than A_0. This is the point where any further increase in A tends to reduce the minimum detectable signal (determining the low end of the dynamic range) at a rate which is greater than the increase at the upper end of the dynamic range, less 30 dB to assure that $b \ll A$ as discussed in Section II. Symbolically,

$$D_m = S_d + A_d - 30 \text{ dB}$$

where S_d is the magnitude of the sensitivity at $A = A_d$. As in the case of Fig. 3, A_d would be increased if reverse self-bias does not occur, giving a corresponding increase in D_m.

The noise corner is reached above $f_m = 30$ kHz since the curves of Fig. 5 are approximately equally spaced as the modulation frequency increases from 100 Hz to 30 kHz. (30 kHz was the largest modulation used since the frequency range of the wave analyzer was limited.) Theoretically, if only $1/f$ noise is involved, the curves of Fig. 5 should be spaced 4.8 dB apart for frequency multiples of 3, and spaced 5.2 dB apart for frequency multiples of 3.33. The slope of the curves in Fig. 5 for $A < A_0$ is approximately -1, which would be expected if the only effect of increasing A is to linearly increase the output [see (3)] without significantly increasing noise. The slope for $A \gg A_0$ is greater than $+1$, which is largely due to the reverse self-bias effect already noted. Finally, A_0 appears very close to the center of the transition region A_{TR} as expected from the earlier discussion in Section II.

B. Schottky Diode

Following the same procedure as previously, the experimental results for the Schottky diode are shown in Figs. 6-8. Fig. 6 shows the minimum detectable signal as a function of A with external bias as a parameter. As before, the curves merge for large A showing that the effect of the external bias is insignificant compared to the rectified RF current due to the large reference signal A. Also note that the curves for different bias levels cross at low levels of A suggesting that at these levels ($A < 30$ dBm) an optimum bias would be less than 100 μA. But this is not the usual laboratory situation since A can generally be set in the transition or linear regions to increase the amplitude of the detected signal without significantly increasing the noise, and to increase the dynamic range. As in the case of the point contact, increasing the bias above 100 μA gave no additional improvement in maximum sensitivity.

Fig. 7 clearly depicts a sharp transition between the square-law and linear regions for all values of external bias. For zero bias the Schottky barely conducts which accounts for the large slope of the zero bias curve, and adding a small amount of bias increases the output of the order of 20 dB for $A \cong -25$ dBm. Another notable feature of Fig. 7 is that the output is independent of A over a range of about 25 dB when bias is present. Among other things, this would have application in automated amplitude measuring systems in which an electronic phase shifter is inserted in the reference branch to sweep the phase angle ϕ through a range of $180°$. The output would vary as $b \cos \phi(t)$, and b could be observed in real time. The unavoidable modulated insertion loss of the phase shifter
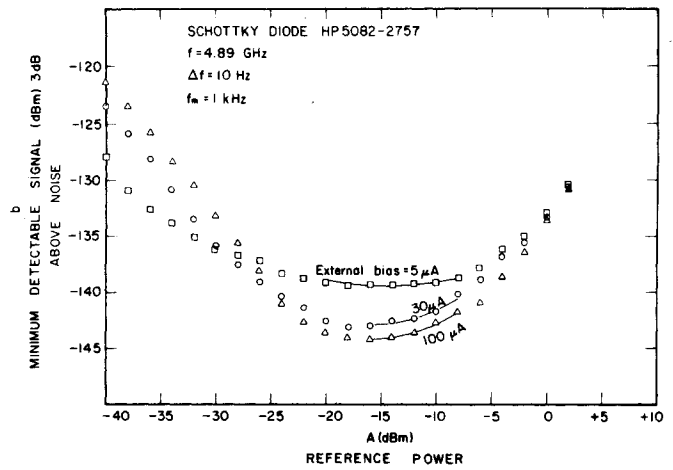

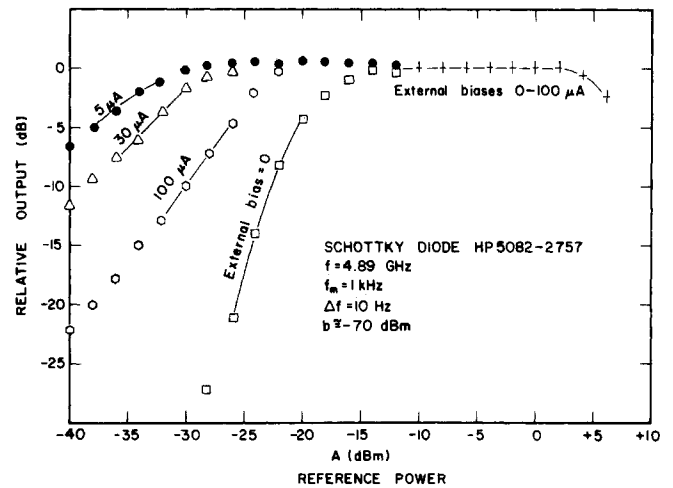Fig. 6. Minimum detectable signal versus A with external bias as parameter for Schottky diode.

Fig. 7. Relative output of Schottky diode versus A with external bias as parameter and fixed information signal input (-70 dBm).
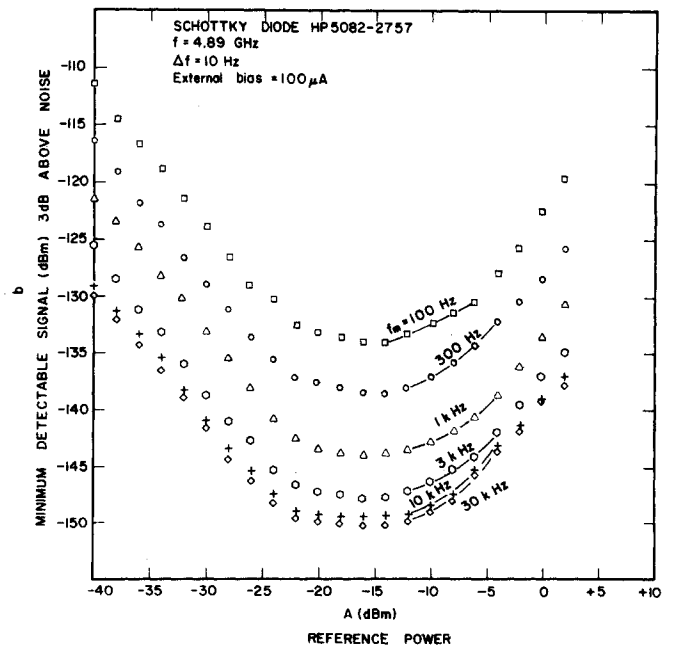

Fig. 8. Minimum detectable signal for Schottky diode versus A with fixed external bias and modulation frequency f_m as parameter.

TABLE II
MAXIMUM SENSITIVITY AND DYNAMIC RANGE AS FUNCTION OF
MODULATION FREQUENCY FOR HP5082-2757 SCHOTTKY DIODE

f_m (Hz)	Maximum Sensitivity S_m (dBm)	A_o (dBm)	Maximum Dynamic Range D_m (dB)	A_d (dBm)
100	-134	-14	96	-6
300	-138	-14	98	-6 to 0
1 k	-144	-16	106	-6 to -2
3 k	-148	-16	108	-6 to -2
10 k	-149	-14 to -18	109	-8 to +2
30 k	-150	-14 to -18	110	-8 to +2

would then contribute insignificant error to the output signal amplitude. Finally, the sharp drop-off for $A > 3$ dBm is due to the onset of severe reverse self-bias which also occurred for the point contact as shown in Fig. 4.

Using 100 μA bias, Fig. 8 displays the behavior of the maximum sensitivity and dynamic range as a function of A and the modulation frequency, and Table II summarizes these results.

Note that the noise corner of the Schottky diode is approached near 10 kHz as evidenced by the bunching of the curves at the higher frequencies. For frequencies below 3 kHz the curves are spread approximately 4.8 or 5.2 dB depending upon the frequency change, which is as expected from the influence of the $1/f$ noise. For $A < A_0$, the slope is steeper than -1 which suggests that the conversion loss increases at low levels of A. At the higher levels, the slope is $+1$ near $A = 0$ dBm, which when compared with Fig. 5 for the point contact, indicates that the upper limit of the dynamic range for the Schottky is about 10 dB greater. In general, comparing Tables I and II, the sensitivity of the Schottky is 15 to 20 dB better than the point contact and the useable dynamic range is increased 20 to 30 dB.

C. Backward Diode

Backward diodes normally operate with zero bias and a very low dc load, and so the only results graphically displayed here are those showing the minimum detectable signal versus A with f_m as a parameter (Fig. 9). The low source resistance of the backward diode required a special transformer input coupled preamplifier which only performed well for $f_m < 3$ kHz, but this was sufficiently high so that a good indication of the system performance could be established. Since the dc impedance of the transformer was only 2 Ω, reverse self-bias was no problem.

When the relative output was measured versus A (not shown), it was found that the device is square law for $A < -6$ dBm, and linear for $A > -2$ dBm, with $A_{TR} \simeq -4$ dBm. Furthermore, the relative output was constant for $-2 < A < +10$ dBm. The experiment was not continued for still larger A because of the danger of burning the diode out. These facts suggest that this diode has a very large dynamic range. Indeed, this can be seen by inspecting Fig. 9 and the summarizing data in Table III.

The most notable features of the data in Fig. 9 are that the point of maximum sensitivity A_0 is much larger than the corresponding points on Figs. 5 or 8 for the point contact or Schottky diodes, respectively. Another is that for $A < -15$
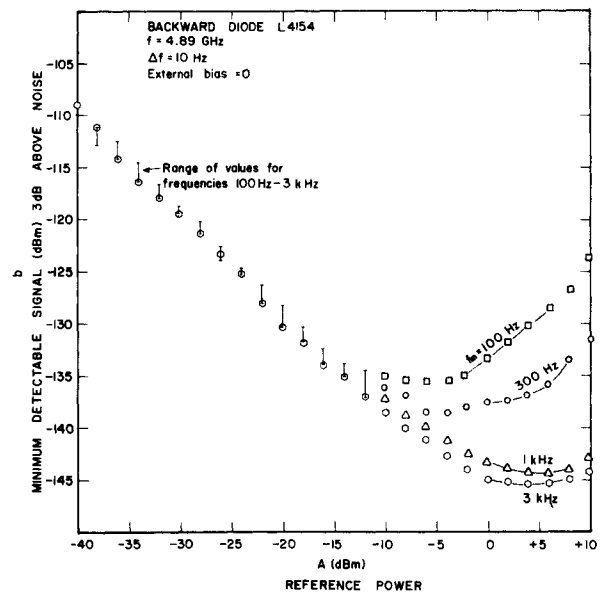

Fig. 9. Minimum detectable signal for backward diode versus A with modulation frequency f_m as parameter.

TABLE III
MAXIMUM SENSITIVITY AND DYNAMIC RANGE AS FUNCTION OF
MODULATION FREQUENCY FOR L4154 BACKWARD DIODE

f_m (Hz)	Maximum Sensitivity S_m (dBm)	A_o (dBm)	Maximum Dynamic Range D_m (dBm)	A_d (dBm)
100	-135	-8 to -4	105	+ 8
300	-138	-6 to -4	112	+6 to +10
1 k	-144	+4 to +6	≥122	> +10
3 k	-145	+2 to +6	≥124	> +10

dBm there is little spread in the curves as would normally be expected from $1/f$ noise. For $A > -15$ dBm, the spread is quite nonuniform which suggests that the noise behaves as $1/f^n$ where $n > 1$. The bunching of the 1-kHz and 3-kHz curves for large A could be due to an approaching noise corner frequency, or perhaps is due to the difference in frequency response of the transformer or different loading effects or a combination of these. Comparing Fig. 9 and Table III with Fig. 8 and Table II shows that the backward diode is capable of providing a dynamic range which is approximately 15 dB greater than that for the Schottky diode, and maximum sensitivities which are approximately equal for the two diodes.

A short final experiment confirmed the fact that the point contact and the Schottky diodes both have a $1/f$ noise spectrum and noise corners greater than 30 kHz and approximately 8 kHz, respectively. The backward diode, however, has a $1/f^{1.5}$ noise spectrum, which was also shown by Eng [17], and a noise corner greater than 3 kHz.

V. CONCLUSION

Since these experiments only involved one diode of each type, generalizations to all other diodes of the same type should be made with some caution. However, trends and certain individual results should be noted.

1) By paying careful attention to the various parameters, optimum sensitivities which greatly exceed previously reported results are possible. Table IV compares these previous data to

TABLE IV
COMPARISON OF HOMODYNE SYSTEM SENSITIVITIES OBTAINED BY
VARIOUS AUTHORS REFERRED TO 10-Hz BANDWIDTH

Author	CW Frequency f	Detector Type	Mod. Freq. f_m in Hz & (Mod. Type)	Sensitivity, S or (Max. Sens., S_m) dBm	Ref. Signal, A or (Opt. Ref.) Signal, A_0 dBm	External Bias
Brodwin, et al., [6]	9 GHz	Point Contact	400 (DSBWC)	(-97)	(-20)	0
			2k (DSBWC)	(-107)	(-20)	0
	24 GHz	IN26 Point Contact	? (DSBWC)	(-115)	(-10)	0
Mathers [7]	X-band	X421A Point Contact	1k (SSBSC)	(-105)	(-15)	0
		Barretter	1k (SSBSC)	-100	0	0
Richmond [8]	X-band	IN23 Point Contact	1k (DSBSC)	(-89)	(-6)	0
		821 Sperry Barretter	1k (DSBSC)	-91	+10	+5 MA
O'Brien [9]	10 GHz	Point Contact	100k (DSBSC)	-130	≈ -3	0
Jaggard & King	4.89 GHz	IN23E Point Contact (table 1)	30k (DSBWC)	(-135)	(-16)	100 µA
		HP5082-2757 Schottky (table 2)	30k (DSBWC)	(-150)	(-18) to (-14)	100 µA
		L4154 Backward (table 3)	3k (DSBWC)	(-145)	(+2) to (+6)	0

the data obtained here. In the Brodwin *et al.* [6] data, the bandwidth was assumed to be 30 Hz since this information was not explicitly given. In all cases, the data are referred to a 10-Hz noise bandwidth.

2) Very large dynamic ranges not available with other conventional detection techniques were also observed. Values of D_m were measured as 92 dB for the point contact at f_m = 30 kHz and 100-µA bias (Table I), 110 dB for the Schottky at f_m = 30 kHz and 100-µA bias (Table II), and 124 dB for the backward diode at f_m = 3 kHz and zero bias (Table III).

3) The optimum reference signal A_0 for point contacts lies in the transition region from square-law to linear detection, while A_0 lies 5-10 dB above this region for Schottky and backward diodes.

4) Below 50 GHz, the Schottky diode is almost an exact replacement for the point contact diode. At modulation frequencies below 10 kHz the Schottky diode can improve homodyne sensitivity by 15 to 20 dB and increase the dynamic range by 20 to 30 dB when compared with the point contact diode (compare Tables I and II). The maximum sensitivities achieved for the point contact and Schottky diodes at 1 kHz compare well with the predicted sensitivities of -127 and -149 dBm, respectively.

If operation is well into the linear region, say A > -15 dBm there is little need for an external bias for either type (see Figs. 4 and 7). Adding a small amount of bias improves the maximum sensitivity slightly as seen from Figs. 3 and 6.

5) The backward diode offers an excellent dynamic range because A_0 is quite large. For f_m = 1 kHz, D_m is 43 dB greater than that of the point contact and the maximum sensitivity of the same order as that for the Schottky (compare Tables I-III). For the system used here, its low IF impedance probably prevented attainment of better sensitivities. Nevertheless, the

maximum sensitivity of -144 dBm at 1 kHz compares with the predicted sensitivity of -153 dBm.

6) The point contact and Schottky diodes both have a clearly defined $1/f$ noise spectrum at low frequencies. The backward diode has a $1/f^{1.5}$ noise spectrum for low frequencies.

For sufficiently narrow bandwidths, homodyne systems operating with audio frequency modulation offer sensitivities which are equal to or greater than those of typical high IF hetrodyne systems which use much wider bandwidths.

Even greater dynamic ranges are possible for the point contact and Schottky diodes if the reverse self-bias effect is reduced or eliminated. Furthermore, D_m can also be significantly increased for all diode types if a balanced modulator or detector is used, allowing removal of the restriction that b/A < -30 dB previously imposed. Perhaps other devices such as the space-charge-limited diode or the hot carrier thermoelectric detector have properties suitable for homodyne systems. These devices have excellent tangential sensitivities and no $1/f$ noise [2].

REFERENCES

[1] R. E. Bayliss, E. Cabrera, and S. E. Howe, "Why a Schottky-barrier? Why a point-contact?," *Microwaves*, vol. 6, pp. 34-45, Mar. 1968.
[2] A. M. Cowley and H. O. Sorensen, "Quantitative comparison of solid-state microwaves detectors," *IEEE Trans. Microwave Theory Tech.*, vol. MTT-14, pp. 588-602, Dec. 1966.

[3] B. S. Siegal, "Schottky diodes—where we stand today," *Microwaves*, vol. 10, pp. 44–46, Apr. 1971.

[4] R. O. Wright, "The backward diode—when and how to use it," *Microwaves*, vol. 3, pp. 22–27, Dec. 1964.

[5] ——, "New twist for backward diode help from low-noise amplifier," *Electronics*, vol. 39, pp. 74–77, July 11, 1966.

[6] M. E. Brodwin, C. M. Johnson, and W. M. Waters, "Low level synchronous mixing," in *IRE Nat. Conv. Rec.*, vol. 1, pt. 10, pp. 52–57, Mar. 1953.

[7] G. W. C. Mathers, "Homodyne generator and detection system," in *IRE Wescon Conv. Rec.*, vol. 1, pt. 1, pp. 194–200, 1957.

[8] J. H. Richmond, "Measurement of time-quadrature components of microwave signals," *IRE Trans. Microwave Theory Tech.*, vol. MTT-3, pp. 13–15, Apr. 1955.

[9] B. B. O'Brien, "A pseudo-superheterodyne receiver for measuring phase and amplitude," *IEEE Trans. Instrum. Meas.*, vol. IM-16, pp. 124–128, June 1967.

[10] G. E. Schafer, "A modulated subcarrier technique of measuring microwave phase shifts," *IRE Trans. Instrum.*, vol. I-9, pp. 217–219, Sept. 1960.

[11] R. J. King, "Real time measurement of microwave parameters and EM fields," *IEEE Trans. Instrum. Meas.*, vol. IM-21, pp. 2–10, Feb. 1972.

[12] B. A. Howarth and T. J. F. Pavlásek, "Analysis of automatic homodyne method amplitude and phase measurements," *IEEE Trans. Microwave Theory Tech.*, vol. MTT-20, pp. 623–626, Sept. 1972.

[13] G. E. Schafer and R. R. Bowman, "A modulated sub-carrier technique of measuring microwave attenuation," *Proc. Inst. Elec. Eng.*, vol. 109B(23), pp. 783–786, May 1962.

[14] W. E. Little, "Further analysis of the modulated subcarrier technique of attenuation measurement," *IEEE Trans. Instrum. Meas.*, vol. IM-13, pp. 71–76, June–Sept. 1964.

[15] H. C. Torrey and C. A. Whitmer, *Crystal Rectifiers*. New York: McGraw-Hill, 1948.

[16] G. C. Messenger and C. T. McCoy, "Theory and operation of crystal diodes as mixers," *Proc. IRE*, vol. 45, pp. 1269–1283, Sept. 1957.

[17] S. T. Eng, "Low-noise properties of microwave backward diodes," *IRE Trans. Microwave Theory Tech.*, vol. MTT-9, pp. 419–425, 1961.

Automatic Test System for an Analog Computer

J. FRANK ROSS, DOUGLAS G. PINCOCK, MEMBER, IEEE, ROBERT J. KAVANAGH, AND DAVID M. WANAMAKER

Abstract—This paper describes the design, construction, and performance of an automatic test system for the analog portion of a hybrid computation system. The system, which is capable of carrying out complete dynamic testing of each analog component, uses the digital portion of the hybrid system to provide the desired control with the result that the requirement for sophisticated stimulation and measurement equipment is minimized. The hardware and software of the system are both modular in nature in order to provide versatility and to facilitate modifications and additions as required. The design philosophy is such that the methods used are not limited to a particular analog computer. In fact, they have applications in the testing of many types of electronic equipment.

I. INTRODUCTION

ONE OF THE MAIN difficulties in making efficient use of hybrid computation systems is the fact that failures in the analog subsystem are relatively frequent. It is, of course, important that such failures be isolated before they introduce errors into solutions. This can be accomplished to a certain extent through extensive use of static checks by programmers [1], [2]. These checks, however, provide no guarantee that components are operative in a dynamic sense, i.e., that integrators do in fact integrate, that nonlinear function generators work in all quadrants, that the frequency response of amplifiers is adequate, etc. Therefore, if users are to have confidence in a hybrid system, it is essential that frequent preventative maintenance tests be carried out on all components. Unfortunately, such tests tend to be very time consuming and hence, are carried out relatively infrequently. Due to the presence of a general-purpose digital computer in the hybrid configuration, it seems natural to investigate the use of automatic testing as a solution to this problem. This paper describes the development of an automatic test system for the analog portion of the EAI 590 Hybrid Computation system at the University of New Brunswick, Fredericton, N.B., Canada.

One of the main considerations in the design of the automatic test system was to minimize costs by using the digital computer as much as possible in place of sophisticated stimulation and measurement equipment. In addition, both hardware and software were designed to be modular in nature in order to provide versatility and facilitate modifications and additions as required.

II. OVERVIEW OF THE TEST SYSTEM

Stuehler [3] divides any general automatic test system into the following logical units, as shown in Fig. 1:

1) a unit which is under test (UUT);